http://bilimseldergiler.atauni.edu.tr/system/index.php/physics-astronomy/index
Atatürk Üniversitesi
Anadolu Fizik ve Astronomi Dergisi
Cilt 1, Sayı 1, 23-30, 2021

Atatürk University
Journal of Anatolian Physics and Astronomy
Volume 1, Issue 1, 23-30, 2021

JAPA

Measurement of the *K*-Shell Fluorescence Cross-Sections, Fluorescence Yields and Transition Rates at 59.54 keV photon energy

Sevil (PORİKLİ) DURDAĞI[*1], Ahmed Hasan Hashim AL- JALAWEE[1], Fatma GÜZEL[1]

[1]Erzincan Binali Yıldırım University, Department of Physics, Faculty of Arts and Science, Erzincan-TURKEY

(Alınış / Received: 12.03.2021, Kabul / Accepted: 21.04.2021, Online Yayınlanma / Published Online: 30.06.2021)

*Corresponding Author: sporikli@erzincan.edu.tr (S. Porikli Durdağı)
(ORCİD: https://orcid.org/0000-0002-4699-2207)

Keywords
X-ray fluorescence, (XRF), Cross-sections, Fluorescence yield.

Abstract: The *K*-shell x-ray fluorescence cross-sections, fluorescence yields and transition ratios are determined experimentally for the elements Fe, Co, Ni, Cu, Zn, Se, Mo, Ag, Gd and Dy at excitation energy of 59.54 keV associated with γ-rays of ^{241}Am radioisotope. *K* x-rays emitted by samples were detected by a Ge(Li) detector with resolution ~160 eV at 59.54 keV. A comparison is made of the experimental results with appropriate theoretical values and other measured values. A good agreement is observed between experimental and theoretical values.

K-Tabakası Flüoresan Tesir Kesitlerinin, Flüoresans Verimlerinin ve Geçiş Hızlarının 59.54 keV Foton Enerjisinde Ölçümü

Anahtar Kelimeler
X-ışını flüoresans, (XRF), Tesir Kesiti, Flüoresans verim.

Özet: Fe, Co, Ni, Cu, Zn, Se, Mo, Ag, Gd ve Dy elementleri için *K*-tabakası x-ışını flüoresans tesir kesitleri, flüoresans verimleri ve geçiş hızları 241Am radyoizotop kaynağından yayımlanan 59.54 keV uyarma enerjisindeki γ-ışınları kullanılarak deneysel olarak belirlenmiştir. Numuneler tarafından yayımlanan *K* tabakası x-ışınları, 59.54 keV'de ~160 eV çözünürlüğe sahip bir Ge(Li) dedektörü tarafından tespit edilmiştir. Deneysel sonuçlarımız uygun teorik değerler ve diğer ölçülen deneysel değerler ile karşılaştırılmıştır. Deneysel ve teorik değerler arasında iyi bir uyum gözlenmiştir.

1. Introduction

The accurate determination of K x-ray transition rates for elements is important because of their widespread use in the fields of atomic, molecular and radiation physics, and in nondestructive elemental analysis by x-ray emission technique, basic studies of nuclear and atomic processes leading to the emission of x-rays and Auger electrons, and dosimetric computations for medical physics and radiation processing. In recent years, many publications have dealt with calculations or measurements of these atomic data. Comparison between experimental and theoretical values is not so clear because they do not take into account the same secondary phenomena. Uncertainties in experimental data are quite large; this is mainly due to the fact that the detectors are not accurately calibrated in this energy range and to do difficulties of making accurate x-ray absorption correction. Due to uncertainties and approximations in the values of these tabulated parameters, users prefer the experimentally measured ones.

Considerable importance in having adequate knowledge of these transition rates concerns the accuracy of the information, which may be obtained about atomic structure. In earlier investigations, studies of the K and L x-ray fluorescence cross-

sections, fluorescence yields and intensity ratios of many elements have been measured by various authors [1,2,3,4,5,6,7,8,9]. Many assessments have been performed in this area in regard to intensity ratios, the most popular being the predictions given by Scofield [10,11]. Scofield [10] used a relativistic Hartree–Slater model to compute K and L-shell x-ray intensity ratios and found out that a relativistic Hartree–Fock approach, including exchange and overlap corrections was needed to reduce discrepancies, of the order of 10%, between theory and experiment. Jankowski and Polasik [12] and Lindgren [13] consider Breit and second order QED (self-energy and vacuum polarization) corrections, not taken into account by Scofield. Martins [14] investigate the effect of the Breit interaction on K_β/K_α ratios and find it negligible. Several experiments have also been performed to study the influence of alloying effect on the K_β/K_α intensity ratios for 3d transition metals.

Vacancies in the shells can be produced by charged particle impact, photoionization, and internal conversion, orbital electron capture or by higher order effects in nuclear decay. In the present method the K shell vacancies are created by photons and filled by outer electrons leading to the emission of K x-rays. We use here the usual x-ray line designations, namely K_α for all K-L transitions and K_β for all K-M and higher shells transitions (the initial state always has a one hole and in the final state the hole is occupied by one of the other electrons).

Earlier experimental K x-ray fluorescence cross-sections were measured using radioisotopes as excitation sources [3,15,16]. They have the advantages of stable intensity and energy and of small sizes, which allow compact and efficient geometry, and they operate without any external power. An alternative to radioisotopes is the use of an x-ray tube with a secondary target arrangement [17].

Some theoretical studies on K XRF cross-sections for several elements at low excitation energies have been reported. Krause et al. [1] have calculated theoretically K XRF cross sections for elements with $5 \leq Z \leq 101$ at photon energies ranging from 10 to 60 keV. Puri et al. [18] have calculated K and L-shell XRF cross sections for elements with $13 \leq Z \leq 92$ and $35 \leq Z \leq 92$ respectively at 1 to 200 keV incident photon energy range. Earlier experimental K x-ray fluorescence cross sections have been measured using radioisotopes as excitation sources [3]. Experimental L x-ray cross sections were measured using radioisotopes as excitation sources [19,20]. Durak et al. [16], Karabulut et al. [9] and Baydaş et al. [21] obtained experimental values of K-shell fluorescence cross sections.

K-shell fluorescence yields w_K for different elements have been investigated for many years. An annotated bibliography of measurements, analysis, fits and tables of K, L and higher atomic shell x-ray fluorescence yield, from 1978 to 1993 were presented by Hubbell et al. [22]. They obtained values of w_K for the elements $11 \leq Z \leq 99$ by fitting the appropriate experimental data and compared these values with the data based on theoretical models presented by Bambaynek et al. [23] and Krause et al. [1].

We have added some more recent measurements of K shell fluorescence cross-sections, fluorescence yields and x-ray transition rates to the collected data cited above. In present work, targets (Fe, Co, Ni, Cu, Zn, Se, Mo, Ag, Gd and Dy) were irradiated by a 241Am radioisotope source. The energy of primary photon that is 59.54 keV yields from 241Am can excite K, L and other shells. Results are compared with experimental results, theoretical predictions and semi empirical fits reported in literature.

2. Materials and Methods

The experimental arrangement and the geometry used in the present study are shown in Fig.1. The experimental setup consists of an energy-dispersive spectrometer in a conventional 45° – 45° geometry.

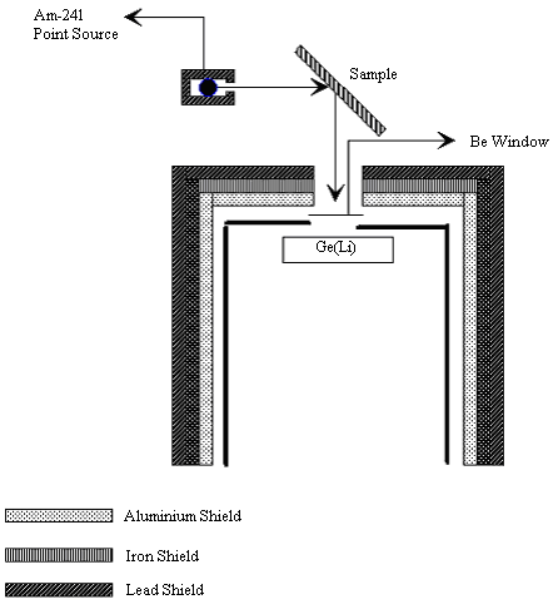

Figure 1. Geometry and shielding arrangement of the experimental setup.

Pure targets of Fe, Co, Ni, Cu, Zn, Se, Mo, Ag, Gd and Dy thickness ranging from 2 to 22 mg/cm2 have been used in this arrangement. Gamma rays of 59.54 keV from 100 mCi 241Am point source were used to ionize the target atoms and the emitted x-rays fallowing the ionization were detected by a Ge(Li) detector having a 25 μm thick beryllium window. The excitation source was housed at the center of cylindrical lead shield of 1 cm diameter and 3.2 cm length. A lead collimator (80 mm length and 5 mm wall thickness) shielded the detector so that only photons from a very small solid angle around the scattering foils could arrive at the

detector. 26.34 keV gamma rays and Np Lα rays coming from 241Am were completely filtered out with the help of graded filters. The graded filters consisting of Pb, Cu and Al were used for the absorption of fluorescent x-rays produced in the filters itself. The resolution of the Ge(Li) detector was ~160 eV [full width at half maximum (FWHM)] for a 5.96 keV x-ray peak.

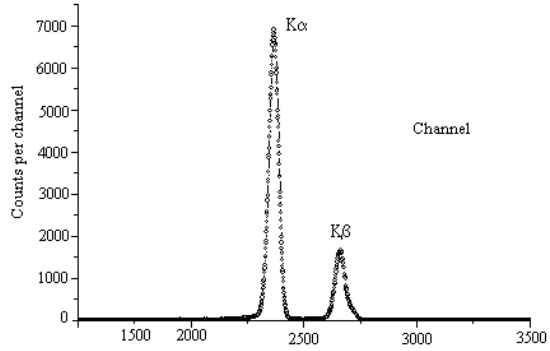

Figure 2. Typical *K* X-ray spectrum for Zn irradiated with 59.54 keV gamma rays from ^{241}Am point source.

Data multichannel analyzer system (ND 66B) consists of 8192 channel analyzers and a spectroscopy amplifier. The live time was taken as 7200 s for all elements. The weighted average of the peak areas was obtained in each case, to reduce statistical error in the measurements. Due to incomplete charge collection in detector and scattering of the photons from the various elements detection system, characteristics peaks contained a low-energy tail, which makes it difficult to obtain the net peak areas. A tail stripping procedure was therefore applied for the spectrum, and after application of this procedure, net peak areas were obtained [24-25]. A typical K x-ray spectrum of Zn is shown in Fig. 2. The peaks due to K_α and K_β peaks are well resolved.

3. Results and Discussion

Measured and generated intensity ratios are related by means of the expression:

$$\left(\frac{I_\beta}{I_\alpha}\right)_{meas} = A\eta\left(\frac{I_\beta}{I_\alpha}\right) \tag{1}$$

where A takes into account the effect of absorption of the incident and K_α and K_β fluorescent radiations and η is the correction for detection efficiency. A dominant interest in techniques based on x-ray analysis is the ratio between the K_α and total K characteristic intensities:

$$\zeta = \frac{1}{1+\frac{I_\beta}{I_\alpha}} = \frac{1}{1+\left(\frac{1}{A\eta}\right)\left(I_\beta/I_\alpha\right)_{meas}} \tag{2}$$

Assessment of A is obtained through use of the well-known expressions for simple (single scattering) events:

$$A = \frac{\beta_{K\alpha}}{\beta_{K\beta}} \tag{3}$$

where $\beta_{K\alpha}$ and $\beta_{K\beta}$ are the self-absorption correction factors for the incident photons and emitted K_i group of $(i = \alpha, \beta)$ x-ray photons.

The detection efficiency for fluorescence lines $(i = \alpha, \beta)$ took into account not only attenuation in the entrance window and layers of the detector, but also for losses due to the finite thickness t_{Ge} of the active Ge layer

$$\begin{aligned}\varepsilon_i = \exp\{-[&\mu_{Be}(E_i)t_{Be} + \mu_{Au}(E_i)t_{Au} \\ &+ \mu_{Ge}(E_i)t_{DL}]\}\mathrm{x}\{1 \\ &- \exp[\mu_{Ge}(E_i)t_{Ge}]\}\end{aligned} \tag{4}$$

where the first exponent accounts for losses in the beryllium window, gold contact and dead layer (DL), and the second exponent represents the probability of a photon being absorbed in the active volume. The corrections $\eta = \varepsilon_\beta/\varepsilon_{\alpha_\alpha}$ on the line ratios in no case exceeded 1%. The measured $\varepsilon_{K\alpha}$ values for the present setup are plotted as a function of the energy in Fig. 3.

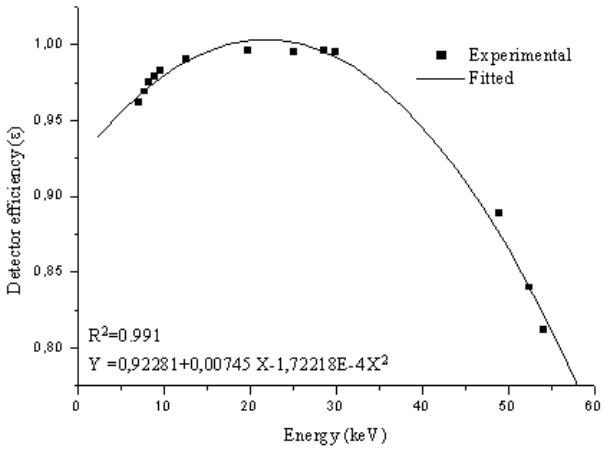

Figure 3. The factor ε_K (theoretical efficiency) as a function of mean *K* X-ray energy.

The values of the experimental K x-ray fluorescence cross-sections can be calculated from the measured quantities using the equation

$$\sigma_{K_i} = \frac{I_{K_i}}{I_0 G \varepsilon_{K_i} \beta_{K_i} t_i} \tag{5}$$

where I_{K_i} is the observed intensity (area under the photopeak in counts per seconds) corresponding to the K_i group of x-rays, I_0 is the intensity of the incident radiation, G is the geometrical factor dependent on the source-sample geometry, ε_{K_i} is the detection efficiency for the K_i group of x-rays, and t is the thickness of the

target in g/cm^2. β is the self-absorption correction factor for the incident photons and emitted K_i group of x-ray photons and is given by

$$\beta_{K_i} = \frac{1 - \exp\{-[\mu(E_0)\sec\theta_1 + \mu_{K_i}(E)\sec\theta_2]t\}}{[\mu(E_0)\sec\theta_1 + \mu_{K_i}(E)\sec\theta_2]t} \quad (6)$$

where $\mu(E_0)$ and $\mu_{K_i}(E)$ are the total mass absorption of the target material for the incident photon and the emitted characteristic x-rays, respectively. The angles incident photons and emitted x-rays with respect to the normal at the surface of the sample θ_1 and θ_2 were equal to 45° in the present setup. The measured $I_0 G \varepsilon_{K_i}$ values for the present setup are plotted as a function of the energy in Fig. 4.

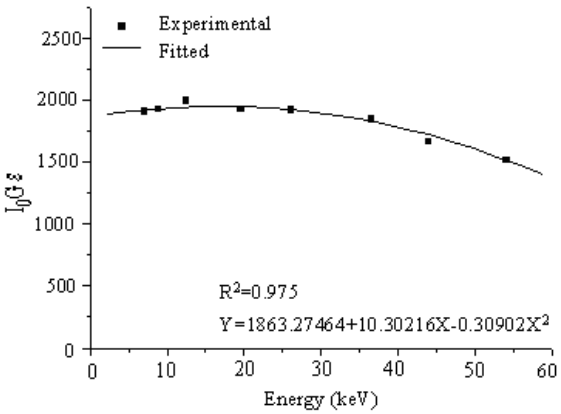

Figure 4. The factor $I_0 G \varepsilon_K$ (experimental efficiency) as a function of mean K X-ray energy.

Theoretical values of σ_{K_i} x-ray fluorescence cross-section were calculated using the equation

$$\sigma_{K_i} = \sigma_K(E_0) w_K \tau_{K_i} \quad (7)$$

where $\sigma_K(E_0)$ is the K-shell photoionization cross-section for the given element of excitation energy E_0, w_K is the K-shell fluorescence yield and τ_{K_i} is the fractional x-ray emission rate for K_i group of x-rays and is defined as

$$\tau_{K\alpha} = \left(1 + {I_{K\beta}}/{I_{K\alpha}}\right)^{-1} \quad (8)$$

$$\tau_{K\beta} = \left(1 + {I_{K\alpha}}/{I_{K\beta}}\right)^{-1} \quad (9)$$

where $I_{K\alpha}$ and $I_{K\beta}$ are the K_α and K_β x-ray intensities, respectively. In the present calculations, the value of $\sigma_K(E)$ was taken from Scofield's values based on Hartree-Slater potential theory[26] and the values of w_K were taken from the tables of Hubbell et al.[22]. Two sets of values IK_β/IK_α were used for evaluation of theoretical K x-ray cross-sections, one based on Hartree-Fock theory [10] and the other on Hartree-Slater theory [11].

First, we measured the K x-ray fluorescence cross-sections for Fe, Co, Ni, Cu, Zn, Se, Mo, Ag, Gd and Dy at excitation energy of 59.54 keV. The theoretical values of the x-ray fluorescence cross-sections have been evaluated by using Eqs. (7). The measured values and theoretical values are given in Table 1 and 2. For comparison, theoretical predictions and measured fluorescence cross-sections are plotted as a function of atomic number in Fig. 5. (a)-(b).

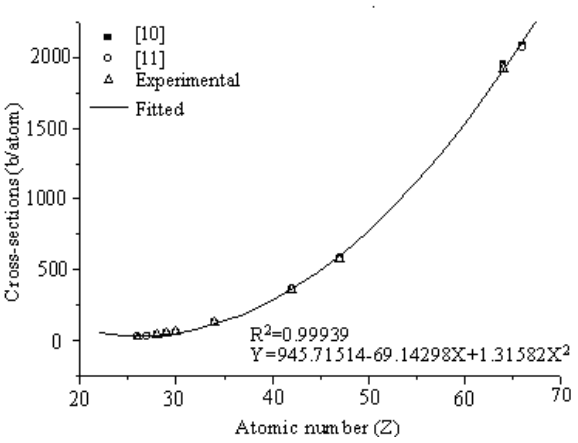

a

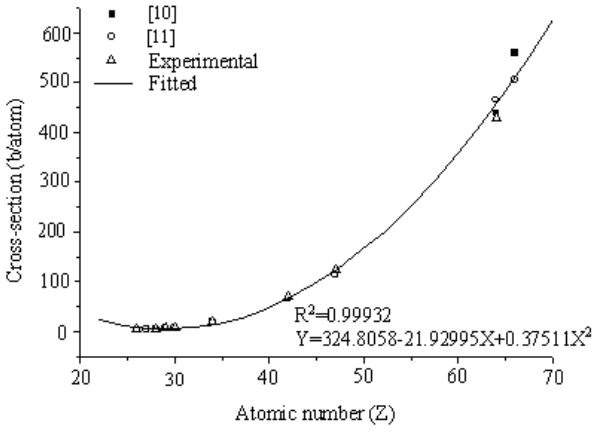

b

Figure 5.a. and b. *Kα* and *Kβ* x-ray fluorescence cross-sections.

In this study, our results are in greater agreement with the theoretical values Scofield's theory [10] based on relativistic Hartree-Fock theory than the theoretical values of Scofield's theory [11] based on the relativistic Hartre-Slater theory model. The disagreement between the experimental and theoretical results can either be due to some systematic error or the error(s) in calculating the physical parameters (σ_{K_i} and τ_{K_i}) used to evaluate the theoretical K x-ray fluorescence cross-sections.

Table 1. Experimental and theoretical K_α x-ray fluorescence cross-sections (b/atom).

		Theoretical values		Experimental values	
Element-Z	**Present work**	**Scofield [10]**	**Scofield [11]**	**Karabulut et al.[9]**	**Durak et al.[27]**
Fe-26	25.936±3.01	26.148	25.728	24.4±1.7	24.64±0.37
Co-27	33.829±4.26	33.425	-	35.8±2.5	-
Ni-28	42.243±5.93	41.890	41.250	-	41.58±1.49
Cu-29	51.916±5.64	52.290	51.540	54.1±5.0	48.06±3.72
Zn-30	61.537±5.16	64.084	63.133	67.1±5.7	64.64±4.36
Se-34	132.974±2.26	129.256	127.044	145±11	-
Mo-42	361.945±5.72	367.251	361.999	374±22	-
Ag-47	581.660±6.34	585.336	577.324	-	595.30±22.29
Gd-64	1950.567±5.33	1939.791	1917.462	-	-
Dy-66	2082.687±3.72	2065.441	-	-	-

Table 2. Experimental and theoretical K_β x-ray fluorescence cross-sections (b/atom).

		Theoretical values		Experimental values	
Element-Z	**Present work**	**Scofield[10]**	**Scofield[11]**	**Karabulut et al.[9]**	**Durak et al.[27]**
Fe-26	3.130±1.86	3.159	3.578	-	3.80±0.06
Co-27	4.606±1.41	4.071	-	-	-
Ni-28	5.879±5.83	5.140	5.780	-	5.87±0.21
Cu-29	6.580±5.45	6.359	7.108	-	7.50±0.53
Zn-30	7.022±5.04	7.953	8.904	-	9.00±0.57
Se-34	18.903±2.27	18.419	20.630	-	-
Mo-42	65.590±1.68	66.436	71.689	69.4±4.1	-
Ag-47	113.690±6.09	114.960	122.972	-	112.01±4.72
Gd-64	439.520±5.23	465.821	429.924	-	-
Dy-66	509.328±3.67	505.827	-	-	-

In addition, these measurements provide an indirect check on physical parameters, such as photoionization cross-sections, K x-ray emission rates and K-shell fluorescence yields. The fluorescence yield, w_K , is defined as the probability that the filling of a K-shell vacancy be followed by a K radiative emission. w_K is important in the calculation of K atomic level widths, K ionizing cross-sections, absorption coefficients, K x-ray emission probabilities and, though these ways, provides information on nuclear transitions. Several major compilations and evaluations of w_K have been published [6,27,28,29], however, w_K was not often measured. Because of the results all mentioned above, in the second part of this study, we measured the fluorescence yield. The measured values of the K-shell fluorescence yield w_K are compared with the other available experimental [27,30] values and semi empirical fits [1,22] in Table 3. They are plotted as a function of the atomic number in Fig. 6. The present experimental results were fitted versus atomic number. The solid lines in Fig. 5. (a)-(b) and Fig. 6. present the fitted values.

Table 3. Present experimental results, semiempirical fits values and literature experimental values of the *K*-shell fluorescence yields.

		Semi-empirical values		Experimental values	
Element-Z	**Present work**	**Hubbell[22]**	**Krause[1]**	**Arora et al.[30]**	**Durak et al.[27]**
Fe-26	0.352±0.012	0.355	0.340	-	-
Co-27	0.374±0.010	0.388	0.373	-	-
Ni-28	0.404±0.058	0.421	0.406	0.394±0.016	0.330±0.005
Cu-29	0.460±0.054	0.454	0.440	0.410±0.018	0.412±0.015
Zn-30	0.479±0.050	0.486	0.474	0.490±0.020	0.482±0.032
Se-34	0.619±0.022	0.602	0.589	-	-
Mo-42	0.757±0.015	0.767	0.765	-	-
Ag-47	0.784±0.060	0.831	0.831	0.857±0.034	0.829±0.038
Gd-64	0.949±0.052	0.932	0.935	-	-
Dy-66	0.951±0.031	0.938	0.941	-	-

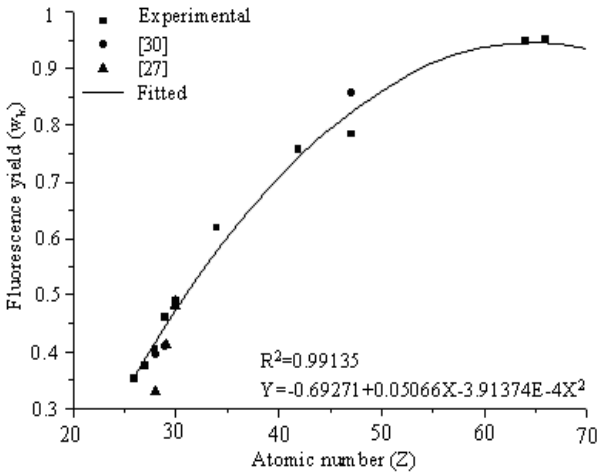

Figure 6.a. Comparison of measured *K*-shell fluorescence yield as a function of the atomic number: Literature experimental results.

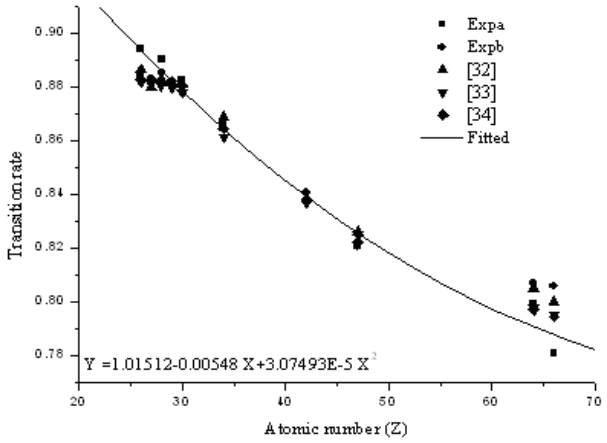

Figure 6.b. Comparison of measured K-shell transition rate as a function of the atomic number: Literature experimental results.

The values of parameters such as fluorescence cross-sections and fluorescence yields need to be measured accurately. The values of these parameters based on Hartree-Slater and Hartree-Fock theory need to be calculated for all elements to check the validity of theory. Due to the agreement between the theoretical and experimental K XRF cross-sections, the measured values can be used with confidence for energy dispersive XRF trace element analysis.

A great deal of work has been carried out in the last few years to improve the K_β/K_α intensity ratio; however, the results are quite similar: there has been no significant improvement in their accuracy. Comparison between experimental and theoretical values is not so clear because they do not take into account the same secondary phenomena, e.g., the K_β/K_α theoretical values [10,11] and the w_K theoretical values [22]. Uncertainties in experimental data are quite large; this is mainly due to the fact that the detectors are not accurately calibrated in this energy range and to the difficulties of making accurate x-ray absorption corrections. In this work, transition rates were determined for two different ways, taking

into account the theoretical detector efficiency values, and taking into account the experimental detector efficiency values. The measured values of transition rates for all the elements studied are given in Table 4 and Table 5. Table 4 and 5 also include theoretical [10,11,31] and previous experimental [32,33,34] results. These values have been plotted as a function of the atomic number and are shown in Fig. 6.a and 6.b.

The overall error is 7-11% in this work. This error arises as a result of uncertainties in the different parameters; namely, the statistical and other possible errors in the area of evaluation of the K x-ray peaks N_K (≤3), errors in the absorption correction factor at incident and emitted photon energies β_{Ki} (≤2), errors in the parameters used to evaluate $I_0 G \varepsilon_{Ki}$ (≤4) and target thickness measurements t (≤2). It can be seen from Table 4 and 5 and Fig. 6.b, that our measurement values are in good agreement, within the experimental uncertainties, with the calculated theoretical values.

Table 5. Present experimental results and theoretical predictions values of the *K*-shell transition rate. Exp[a]: Values calculated using experimental detector efficiency, Exp[b]: Values calculated using experimental detector efficiency.

	Present work		Theoretical values		
Element-Z	**Exp.[a]**	**Exp.[b]**	**Scofield[10]**	**Scofield [11]**	**Manson[31]**
Fe-26	0.8940±0.014	0.8839±0.013	0.8922	0.8779	0.8811
Co-27	0.8820±0.011	0.8830±0.011	0.8914	-	-
Ni-28	0.8900±0.076	0.8850±0.064	0.8907	0.8771	0.8803
Cu-29	0.8812±0.071	0.8816±0.059	0.8916	0.8788	-
Zn-30	0.8822±0.068	0.8822±0.055	0.8896	0.8764	0.8787
Se-34	0.8664±0.023	0.8653±0.023	0.8753	0.8603	0.8643
Mo-42	0.8403±0.016	0.8403±0.016	0.8468	0.8347	0.8354
Ag-47	0.8203±0.077	0.8203±0.066	0.8358	0.8244	-
Gd-64	0.7992±0.068	0.8068±0.048	0.8048	0.7956	0.7958
Dy-66	0.7806±0.031	0.8057±0.031	0.8033	-	0.7956

Table 6. Comparison of present experimental results and literature experimental values of the *K*-shell transition rate.

	Present work		Experimental values		
Element-Z	**Exp.[a]**	**Exp.[b]**	**Hansen *et al.*[32]**	**Khan *et al.*[33]**	**Ertuğrul *et al.*[34]**
Fe-26	0.8940±0.014	0.8839±0.013	0.8863	0.8818	0.8826
Co-27	0.8820±0.011	0.8830±0.011	0.8795	0.8811	0.8826
Ni-28	0.8900±0.076	0.8850±0.064	0.8828	0.8803	0.8811
Cu-29	0.8812±0.071	0.8816±0.059	0.8819	0.8795	0.8818
Zn-30	0.8822±0.068	0.8822±0.055	0.8809	0.8780	0.8803
Se-34	0.8664±0.023	0.8653±0.023	0.8687	0.8613	0.8643
Mo-42	0.8403±0.016	0.8403±0.016	0.8382	0.8368	0.8382
Ag-47	0.8203±0.077	0.8203±0.066	0.8258	0.8251	0.8217
Gd-64	0.7992±0.068	0.8068±0.048	0.8048	0.7975	0.7968
Dy-66	0.7806±0.031	0.8057±0.031	0.7999	0.7949	0.7943

4. Conclusion

In this study, our results are in greater agreement the theoretical values of Scofield's theory [10] based on relativistic Hartree-Fock theory than the theoretical values of Scofield's theory [11] based on the relativistic Hartree-Slater model. The agreement between the present results and theoretical predictions are within the range 0.1-2.8% for theoretical detector efficiency values and 0.07-2.1% for experimental detector efficiency values.

In conclusion, the agreement we find here between the theoretical and experimental values leads to the conclusion that the data presented here will benefit those using the radioisotope XRF technique because of their use in applied fields such as radiation transport in matter, absorbed-dose and radiation effect determinations, trace elemental analysis using either traditional photon sources or synchrotron radiation.

References

[1] Krause MO, J. Phys. Chem. Ref. Data. 1979; 8**,** 307.
[2] Perujo A, Maxwell J, Teesadale W, Campbell JL, J. Phys. B,1987; 20, 4973-4982.
[3] Porikli S, , Demir D, Kurucu Y, Europ. Phys. Jour. D, 2008; 47, 315
[4] Rao DV, Cesareo R, Gigante GE, L Phys. Scrip., 1995; 51:2, 252.
[5] Porikli S, Chemıcal physics letters, 2011; 508, 165.
[6] Horakeri LD, Hanumaiah B, Thontadarya SR, X-ray Spectrom., 1997; 26, 69.
[7] Durak R, Erzeneoğlu S, Kurucu Y, Şahin Y, Radiat. Phys. Chem., 1998; 51, 45.
[8] Bé MM, Lépy MC, Plagnard J, Duchemin B, Appl. Radiat. Isot., 1998; 49, 1367.
[9] Karabulut A, Budak G, Demir L, Şahin Y, Nucl. Instr. and Meth. In Phys. Res. B, 1999; 155, 369.
[10] Scofield JH, Phys. Rev. A, 1974; 9, 1041.
[11] Scofield JH, Atomic Data Nucl. Data Tables, 1974; 14, 121.
[12] Jankowski K, Polasik M, J. Phys. B, 1989; 22, 2369.
[13] Lindgren I, Persson H, Salomaonson S, Karasiev V, Labzowsky L, Mitrushenkov A, Tokman M, J.Phys. B: At. Mol. Opt. Phys. 1993; 26, 503.
[14] Martins MC, Marques MI, Parente F, Frereira JG, J. Phys. B: At. Mol. Opt. Phys., 1989; 22, 3167.
[15] Chang CN, Su WH, Nucl. Instr. and Meth., 1978, 148, 561.
[16] Durak R, Erzeneoğlu S, Kurucu Y, Şahin Y, Instrumentation Science and Technology, 1997, 25, 335.
[17] Singh S, Rani R, Metha D, Singh N, Mangal PC, Trehan PN, , 1990; 19, 155.
[18] Puri S, Chand B, Mehta D, Garg M L, Singh N, Trehan, Atom Data and Nucl. Data Tables, 1995; 61, 289.
[19] Al-Saleh KA, Saleh NS, L Radiat. Phys. Chem., 1999; 54, 117
[20] Demir L, Şahin M, Kurucu Y, Karabulut A, Şahin Y, Radiat. Phys. Chem., 2003, 67, 605.
[21] Baydaş E, Şahin Y, Büyükkasap E, J Quantitative Spectroscopy, 2003; 77, 87.
[22] Hubbell JH, Trehan PN, Singh N, Chand B, Metha D, Garg ML, Garg RR, Singh S, Puri SJ, Phys. Chem. Ref. Data, 1994; 23, 339.
[23] Bambynek W, Crasemann B, Fink RW, Freund HU, Mark H, Swift CD, Price RE, Rao PV, Rev.Mod. Phys. 1972; 44, 716.
[24] Şahin Y, Durak R, Kururcu Y, Erzeneoğlu S, J Radional. Nucl. Chem. Articles, 1994; 177, 403.
[25] Durdağı (Porikli) S, Spec. and spec. Anal., 2018; 38, 2630.
[26] Scofield JH, Report UCRL 51326 Lawrence Livermore Laboratory Livermore, CA 1973.
[27] Durak R, Özdemir Y, Radiat. Phys. Chem., 2001; 61, 19.
[28] Kaya A, Ertuğrul M, J Electron Spectroscopy, 2003; 130, 111.
[29] Yashoda T, Krishnaveni S, Gowda S, Umesh TK, Gowda R, Indian Academy of Sciences 2002; 58, 31.
[30] Arora SK, Allawadhi KL, Sood BS, Physica C, 111, 71.
[31] Manson ST, At. Data Nucl. Data Tables, 1974; 14, 111.
[32] Hansen JS, Freund HU, Fink RW, Nucl. Phys. A, 1970; 142, 604.
[33] Khan MR, Karimi M, X-Ray Spectrom, 1980; 9, 32.
[34] Ertuğrul M, Söğüt M, Şimşek Ö, Büyükkasap E, J. Phys. B: At. Mol. Opt. Phys., 2001; 34, 909.